

Two-Step Reaction on a Strained, Nanoscale Segmented Surface

C. Africh,^{1,2} F. Esch,² W. X. Li,³ M. Corso,^{1,2} B. Hammer,³ R. Rosei,^{1,2} and G. Comelli^{1,2}

¹Physics Department and Center of Excellence for Nanostructured Materials, Trieste University, I-34127 Trieste, Italy

²TASC-INFM Laboratory, I-34012 Basovizza, Trieste, Italy

³Interdisciplinary Nanoscience Center (iNANO) and Department of Physics and Astronomy, University of Aarhus, DK-8000 Aarhus C, Denmark

(Received 16 February 2004; published 16 September 2004)

By means of scanning tunneling microscopy and density functional theory calculations we demonstrate that on the Rh(110)-(10 × 2)-O surface, a prototypical multiphase surface of an oxidized transition metal model catalyst, water formation upon H₂ exposure is a two-step reaction, with each step requiring special active sites. The 1st step initiates at (2 × 1)p2mg-O defect islands in the (10 × 2) structure and propagates across the surface as a reaction front, removing half of the adsorbed oxygen. The oxygen decorated Rh ridges of the (10 × 2) structure lose their tensile strain upon this reduction step, whereby nanoscale patches of clean Rh become exposed and act as special reaction sites in the 2nd reaction step, which therefore initiates homogeneously over the entire surface.

DOI: 10.1103/PhysRevLett.93.126104

PACS numbers: 82.65.+r, 68.37.Ef, 68.43.Bc, 82.30.-b

High coverage, compressed oxygen structures, which often form on transition metal surfaces, can be regarded as the link between the adsorption regime and oxide phases. Recent studies on these thin surface oxides revealed complex geometrical structures and properties which do not have an analogue in bulk oxides (Ru [1], Ag [2], Pd [3,4]). The investigation of their reactivity is therefore a key step towards the understanding of the active phase in catalysis by oxidized transition metals. For surface reactivity studies at the atomic level, scanning tunneling microscopy (STM) was shown to be the technique of choice [5–7].

On Rh(110), a new metastable structure with (10 × 2) periodicity has recently been discovered under high oxygen exposures [8]. In this structure (see Fig. 1), which forms on the (1 × 2) reconstructed substrate, oxygen atoms adsorb on both sides of the top layer metal rows with a total coverage of about two oxygen atoms per ridge Rh atom. The high oxygen coverage induces strain along the Rh ridges, which leads to the ejection of Rh atoms (on the average, two out of ten), leaving behind segments of eight Rh ridge atoms separated by ridge vacancies (RVs). The Rh ridge segments are expanded by ~1/9 in the [1 $\bar{1}$ 0] direction and the oxygen atoms therefore bind in very different local geometries along the segments (see Fig. 1). Lateral interactions between the segments, most likely of an elastic nature, cause the RVs on different ridges to line up in the [001] direction [8]. The ejected Rh atoms form small regions where oxygen adsorbs in the (2 × 1)p2mg-O structure [9]. The (10 × 2)-O surface is therefore a mixture of reconstructed (R) and unreconstructed (UR) areas. Moreover, the nanostructured character of the (10 × 2)-O structure is ideal to investigate the influence of special sites on reactivity, since any special site in the structure will be present in a repeated array throughout the surface.

In this Letter, we present a detailed joint STM and density functional theory (DFT) study of the reactivity of the Rh(110)-(10 × 2)-O surface towards molecular hydrogen. We demonstrate that the reaction proceeds in two distinct steps, governed by two completely different mechanisms. In the 1st step, half of the oxygen is removed from the surface by a reaction front. Only in a 2nd, slower step, which starts homogeneously from the RVs all over the surface, is the remaining oxygen reacted off. The reaction front in the 1st reaction step results from the lack of sites for H₂ dissociation within the fully oxygen covered segmented structure. The homogeneity of the 2nd

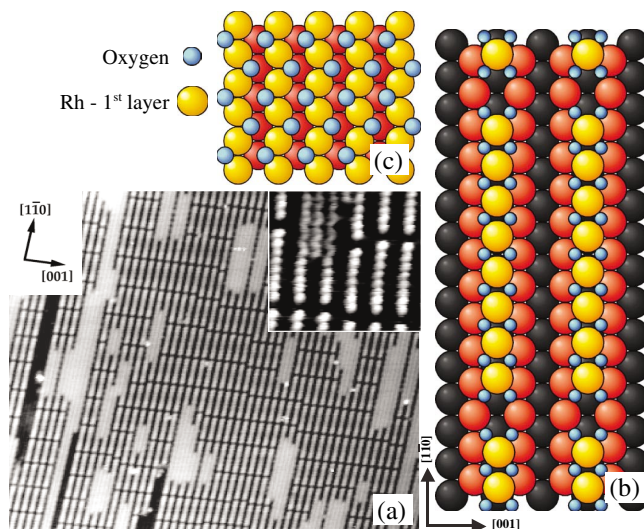


FIG. 1 (color online). STM image and models of the structures present on the (10 × 2)-O/Rh(110) surface: (a) STM image (40 × 30 nm², 1 nA, +0.6 V). In the inset (5.7 × 5.4 nm², 0.54 nA, +0.19 V) atomically resolved zoom on both R and UR areas; (b) model of the R (10 × 2)-O structure; (c) model of the UR (2 × 1)p2mg-O structure.

reaction step is due to the homogeneous appearance of reaction sites after the passage of the reaction front. These sites are shown to be the widened RVs that result as a consequence of the segments losing their strain upon partial reduction.

The (10×2) -O structure was prepared starting from the $(2 \times 2)p2mg$ -O phase [9]. On this surface, an additional 29 langmuir (L) of O_2 were dosed at 200 K; the sample was then annealed to 530 K. STM image series were acquired at room temperature with an Omicron VT-STM, while the surface was exposed to an effective H_2 pressure of 1×10^{-8} mbar (corrected for the tip screening factor [10]). Acquisition times ranged between 18 and 162 s per image; typical scanning parameters were +0.6 V and 1 nA.

Figure 2(a) shows the initial surface [11]. After starting hydrogen exposure, a reaction front propagates over the surface [Fig. 2(b)]. The reaction front alters the super structure of the segments: the segment lengths become irregular and the RVs are no longer aligned. Furthermore, the measured Rh-Rh distance along $[1\bar{1}0]$ within the segments shows that the strain found at the highest oxygen coverage is no longer present. This is consistent with the RVs being enlarged in the $[1\bar{1}0]$ direction. Closer inspection of the STM images [Fig. 2(c)] reveals that the reacted segments appear zigzagged. This is a fingerprint of the presence of oxygen atoms in alternate threefold sites, as in the $(2 \times 2)p2mg$ -O structure [10,12], thus indicating that only half of the initial oxygen is removed in the 1st reaction step. Moreover, the STM image series allows one to see how the reaction proceeds along each segment, removing sequentially one oxygen per couple, starting from a RV [Fig. 2(d)]. The evolution of irregular segment lengths after passage of the reaction front is due to Rh atom diffusion between segments in the $[1\bar{1}0]$ direction. At room temperature, this is the only moment where the substrate atoms move.

The remaining oxygen is removed in a 2nd step, which involves a completely different mechanism. The reaction now starts homogeneously all over the surface from the RVs on [Fig. 2(e); reacted parts appear brighter, as previously observed [12]] and proceeds through a vacancy diffusion process, propagating from each RV towards the center of the segment, until a clean surface is obtained, as judged from the very few residual zigzag oxygen atoms visible in the STM images [Fig. 2(f)] [11]. In this 2nd step, the starting surface closely resembles the $(2 \times 2)p2mg$ -O structure, except that in the present case the close-packed Rh rows are segmented. The segmentation is crucial for the reactivity of the surface. Without segmentation, i.e., on the $(2 \times 2)p2mg$ -O surface, the reaction is almost hindered at room temperature, nucleating exclusively at the few existing defects, e.g., steps. On the segmented structure the reaction can nucleate in all RVs, which act as abundant ministepped, whereby it becomes much faster. The reaction mechanism, however, is the

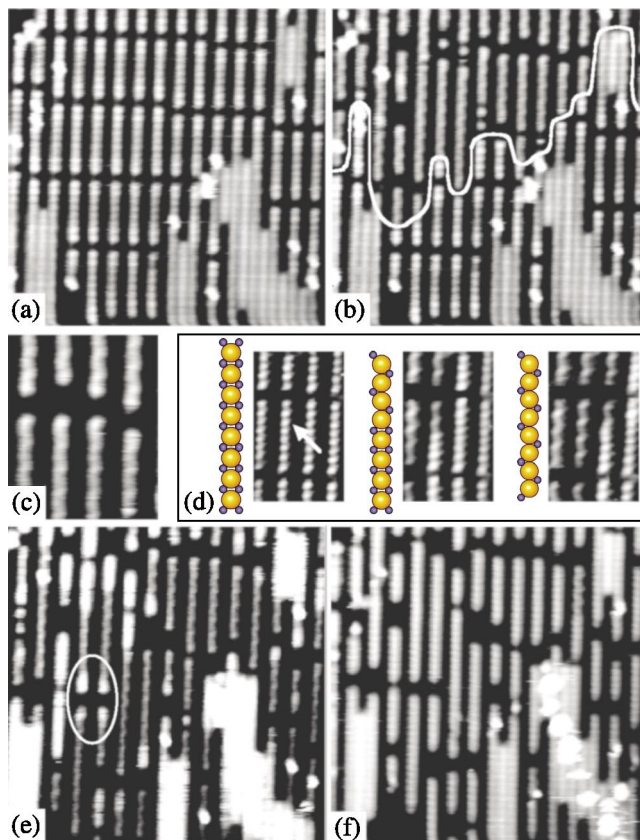


FIG. 2 (color online). STM images of the two reaction steps on a (10×2) -O surface reacting with H_2 at room temperature ($p_{H_2} = 1 \times 10^{-8}$ mbar): (a) initial surface; (b) 1st reaction step: the wave front (white line) propagates over the surface (time needed to cross the imaged area: four images with 18 s/image); (c) enlarged area of the reacted region, showing the remaining O in zigzag threefold sites; (d) propagation of the reaction along a single segment (marked by the arrow); (e) 2nd reaction step proceeding from the segment ends all over the surface (reacted parts appear brighter, as highlighted by the circle); (f) final clean, segmented (1×2) surface (bright features in the bottom right corner are mobile Rh atoms moved to the upper terrace during the 1st reaction step). Dimensions: (a), (b), (e), and (f) 15×15 nm²; (c) 4×5 nm²; (d) 3.6×6.0 nm². Scanning parameters: (a)–(c), (e)–(f) 1 nA, +0.6 V; (d) 0.86 nA, +0.25 V. Time: (a)–(b) 54 s; (b)–(e) 198 s; (e)–(f) 648 s; between images in (d) 35 s.

same, with nucleation at defects and propagation through oxygen vacancy creation and diffusion.

Having demonstrated the two-step character of the water formation reaction, we return to the nucleation event of the reaction front in the 1st reaction step. By analyzing a large number of STM images, we observe that the reaction always starts on a wide UR area of the surface, where it behaves exactly as on the pure $(2 \times 1)p2mg$ -O UR layer. As shown in Fig. 3(a), its onset is evidenced by the formation of oxygen pairs, which gradually cover the area in a 0.5 ML coverage structure. Only after the whole UR region is covered by O pairs [Fig. 3(b)] can the wave front attack the strained (10×2) -O surface [Fig. 3(c)],

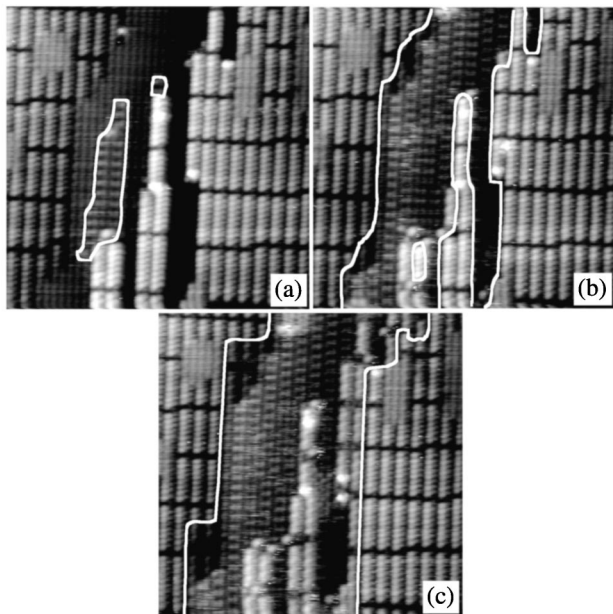


FIG. 3. Onset of the reaction at room temperature. The reaction starts as a front on an UR area, beginning from a step. In the wave front, oxygen is partially reacted off, forming a structure composed of paired oxygen atoms ($\Theta_{\text{O}} = 0.5 \text{ ML}$). White lines separate reacted from unreacted areas. (a) Initial stage of the reaction. (b) UR area completely covered by pairs of O atoms. (c) Onset of the reaction on the strained surface. Parameters: $20 \times 20 \text{ nm}^2$, 0.9 nA , $+0.25 \text{ V}$, 35 s/image . Time: (a)–(b) 280 s ; (b)–(c) 140 s .

while further reaction occurs in the UR region. This indicates that a pure strained $(10 \times 2)\text{-O}$ surface, without UR regions, would be unreactive at room temperature. After its onset, the reaction propagates as a wave front on the unreacted regions, both R and UR.

A previous STM study has described the formation of a front in the water formation reaction on the Pt(111) surface below 170 K as due to an autocatalytic process involving the migration of water molecules [13,14]. In our case, however, water desorbs immediately, and a similar explanation cannot hold. The different mechanism in the two reaction steps (reaction front and homogeneous reaction starting from RVs) can instead be rationalized by the different dissociation probability of molecular hydrogen: on the initial, strained surface, H_2 molecules cannot dissociate. After the 1st reaction step, instead, the H_2 molecules can dissociate in the RVs, enlarged by the strain removal in the reduced Rh ridge segments, and in the troughs of the unstrained, 0.5 ML oxygen covered surface. The 1st reaction step proceeds therefore as a front, with the hydrogen dissociation blocked ahead of it and occurring in the areas behind it. The formation of free adsorption sites for hydrogen dissociation is thus the autocatalytic step.

This reaction mechanism is strongly supported by our DFT investigations. In Fig. 4 (top panel), we present the reaction energy diagrams for H_2 dissociation and subse-

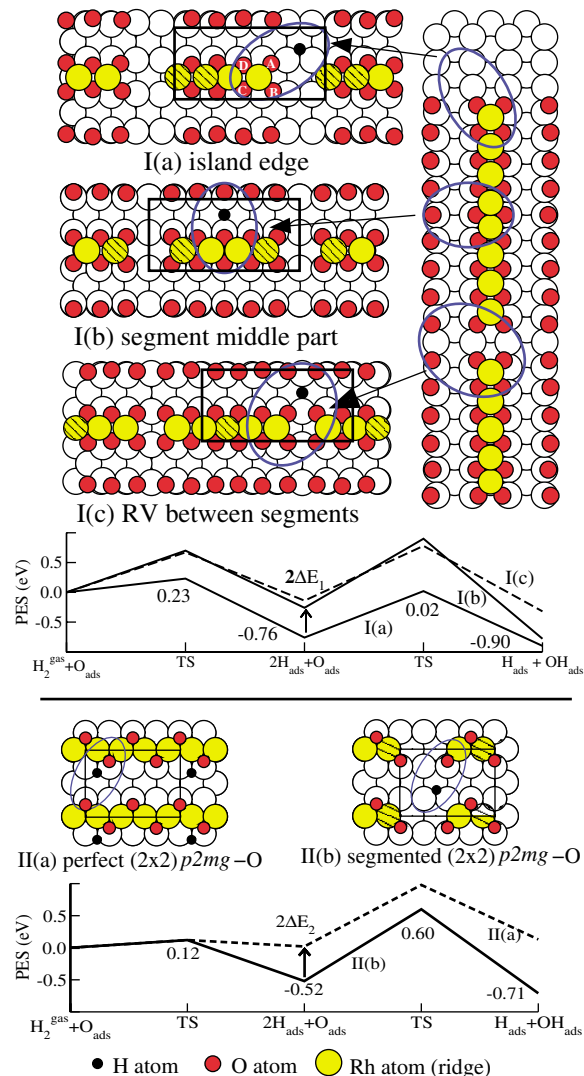


FIG. 4 (color online). Surface models used for DFT calculations and resulting potential energy surfaces (PES) (calculated using the revised Perdew, Burke, and Ernzerhof general gradient approximation [16]) for the 1st (top) and 2nd (bottom) reaction steps. For the 1st reaction step, H_2 dissociation and OH formation were studied on $(10 \times 2)\text{-O}$ at the island edge [I(a)], segment middle parts [I(b)], and RVs [I(c)]. In all cases, models with (6×2) periodicity (indicated by rectangles) have been used. The arrow indicates the adsorption energy difference ($\Delta E_1 = 0.25 \text{ eV/atom}$) for I(a) and I(b) H atoms. For the 2nd reaction step, H_2 dissociation and OH formation were studied at perfect [II(a)] or segmented [II(b)] $(2 \times 2)\text{p}2\text{mg-O}$ surfaces. The arrow indicates the adsorption energy difference ($\Delta E_2 = 0.27 \text{ eV/atom}$) for II(a) and II(b) H atoms. In both panels, the relevant areas are highlighted by ellipses. In order to better mimic the surface, the position of some ridge Rh atoms (hatched) is kept fixed along $[1\bar{1}0]$. The supercell consists of five metal layers (three bottom layers fixed).

quent OH formation at three different models of reaction sites on the fully O covered (10×2) structure. Models I(a), I(b), and I(c) describe the island edge, the segment middle parts, and the RVs, respectively. The barrier for H_2 dissociation is calculated to be 0.23 eV at

the island edge, while inside the structure it is as high as 0.67 eV. In the subsequent OH formation step, the barrier is also smaller at the edge of the (10×2) structure (0.78 eV) compared to sites inside the structure (0.92 and 1.16 eV). The reason for the lower reaction energy barriers at the island edge is the occurrence of a sufficiently large ensemble of clean Rh atoms (not binding to O). This can be asserted by comparing to the reactivity of the clean Rh(110) surface, for which we calculate an H_2 dissociation barrier of 0.09 eV. The calculations therefore suggest that as the segments are reduced starting from the island edge, new ensembles of less oxidized Rh atoms propagate along the segments, thereby constituting the reaction front. The zigzag structure that evolves after passage of the reaction front can be understood in terms of the thermodynamics of the oxygen adsorption along the Rh ridge. The binding of the 1st oxygen atom at the island edge [atom A in Fig. 4 (top)] is calculated to be 1.85 eV. Once this atom is removed, the binding of the nearby oxygen atoms on the same segment (1.85, 1.36, and 1.98 eV for atoms B, C, and D in the figure, respectively) clearly favors the removal of the oxygen atom matching the zigzag pattern.

Once a segment has been reduced to the zigzag structure with half of the oxygen content, the strain is removed and the RV at the reaction front expands. With this larger ensemble of clean Rh atoms, the reaction can propagate across the RV onto the next segment. According to our calculations, H_2 cannot dissociate on the O-saturated Rh atoms ahead of the reaction front, and neither can atomic hydrogen, originating from H_2 dissociating behind the reaction front, diffuse across the front to form OH deep inside the (10×2) structure. As shown by an arrow in the energy diagram in Fig. 4 (top), this would require overcoming an activation barrier at least $\Delta E_1 = 0.25$ eV/atom larger than the 1.16 eV barrier to form OH starting from the hydrogen present in front of the reaction front.

Finally, modeling the conditions for the 2nd reaction step [Fig. 4 (bottom panel)], we find H_2 dissociation energy barriers around 0.12 eV both for the enlarged RVs and the troughs between two reduced, unstrained segments [modeled as the $(2 \times 2)p2mg$ -O structure], indicating that H_2 can dissociate everywhere. However, the potential energy surface shows that H atoms can only adsorb at the enlarged RVs ($\Delta E_2 = 0.27$ eV/atom), which are therefore the active sites for OH formation. Our DFT results thus corroborate the STM observation that the enlarged RVs act as special sites for the 2nd step of the water formation reaction on Rh(110)- (10×2) -O. Since the enlarged RVs are present homogeneously over the entire surface, the 2nd reaction itself becomes homogeneous.

It will be important to verify whether the two-step mechanism we observe for the water production reaction

on Rh(110) has general character, i.e., whether it applies to other reactions where partial removal of the adsorbate layer leaves the residual atoms in a thermodynamically more stable configuration while forming new active sites on the surface. As an example, a remarkable similarity is observed with the water formation reaction on Ru(0001). A previous work, focused on the reaction kinetics, found that the reaction, taking place in the same temperature range, shows a distinct change in the water production rate when the oxygen surface coverage is halved, due to the possibility for hydrogen to dissociate [15].

In conclusion, by comparison of STM imaging and DFT calculations, we demonstrate that the catalytic oxidation of hydrogen on (10×2) -O/Rh(110) starts in the UR areas of the structure and proceeds in two steps. In the 1st step, a reaction front crosses the surface, removing half of the oxygen and leaving the remaining atoms in zigzag threefold sites along the substrate segments, which become unstrained and therefore separated by enlarged RVs. On the resulting surface, H_2 can dissociate everywhere, but H atoms reside only in the enlarged RVs, from which OH formation takes place. The 2nd reaction step thus starts homogeneously from all RVs at the surface.

This work was supported by Regione Friuli Venezia Giulia (L.R. 3/98), by INFM (PAISS CHEMDE), by MIUR (PRIN 2003 and FIRB 2001), and by the Danish Research Councils. Computational resources were provided by Dansk Center for Scientific Computing.

-
- [1] H. Over *et al.*, *Science* **287**, 1474 (2000).
 - [2] C.I. Carlisle *et al.*, *Phys. Rev. Lett.* **84**, 3899 (2000).
 - [3] E. Lundgren *et al.*, *Phys. Rev. Lett.* **88**, 246103 (2002).
 - [4] E. Lundgren *et al.*, *Phys. Rev. Lett.* **92**, 046101 (2004).
 - [5] X.C. Guo and R.J. Madix, *J. Phys. Chem. B* **107**, 3105 (2003).
 - [6] J. Wintterlin, *Adv. Catal.* **45**, 131 (2000).
 - [7] P.T. Sprunger *et al.*, *Surf. Sci.* **344**, 98 (1995).
 - [8] E. Vesselli *et al.*, *J. Chem. Phys.* **114**, 4221 (2001).
 - [9] G. Comelli *et al.*, *Surf. Sci. Rep.* **32**, 165 (1998).
 - [10] C. Africh *et al.*, *J. Chem. Phys.* **115**, 477 (2001).
 - [11] See EPAPS Document No. E-PRLTAO-93-009438 for Fig. 2 STM images—complete movie. A direct link to this document may be found in the online article's HTML reference section. The document may also be reached via the EPAPS homepage (<http://www.aip.org/pubservs/epaps.html>) or from <ftp.aip.org> in the directory /epaps/. See the EPAPS homepage for more information.
 - [12] C. Africh *et al.*, *J. Chem. Phys.* **116**, 7200 (2002).
 - [13] C. Sachs *et al.*, *Science* **293**, 1635 (2001).
 - [14] C. Sachs *et al.*, *J. Chem. Phys.* **116**, 5759 (2002).
 - [15] M.H. Koch, P. Jakob, and D. Menzel, *Surf. Sci.* **367**, 293 (1996).
 - [16] B. Hammer, L.B. Hansen, and J.K. Nørskov, *Phys. Rev. B* **59**, 7413 (1999).